Machine-Learned Electrostatic Potentials for Accurate Hydration Free Energy Calculations

JCTC Journal of Chemical Theory and Computation

pubs.acs.org/JCTC Article

Machine-Learned Electrostatic Potentials for Accurate Hydration Free Energy Calculations

Mathias Hilfiker, Leonardo Medrano Sandonas, Alexandre Tkatchenko, Ola Engkvist, and Marco Klähn*

Cite This: J. Chem. Theory Comput. 2026, 22, 4481−4492 Read Online

ABSTRACT: Free energy calculations are widely used tools in computational chemistry, but their dependence on the assignment of partial charges during force field parametrization reduces their accuracy and reproducibility. In this work, we highlight the direct connection between the low accuracy of AM1-BCC charges on polar species and the poor accuracy of corresponding hydration free energy calculations. We then propose an XGBoost regressor trained on atomic descriptors to rapidly predict charges obtained with high-fidelity density functional theory calculations at PBE0-D3(BJ)/def2-TZVP level. The more accurate electrostatic description results in more reliable free energy calculations than those obtained with semiempirical AM1-BCC charges. Finally, we leverage this predictive model in combination with a 1 ns gas-phase molecular dynamics simulation to propose the Boltzmann Percentile method for assigning charges representative of the conformational ensemble of a molecule. Charges obtained with this method are robust to different input conformations, and the resulting free energies, calculated on a subset of the FreeSolv data set, show a root mean squared error of 1.69 kcal/mol against the 3.05 kcal/mol obtained with semiempirical charges as well as a significantly better ranking. We provide a trained model, easily integrable into traditional workflows, enabling free energy calculations at the same computational cost as AM1-BCC charges. These two aspects make it a realistic tool for enhancing already expensive free energy calculations, and more in general, molecular dynamics simulations in condensed phase.

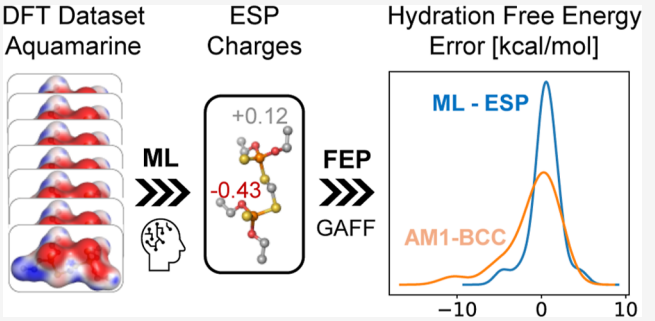

INTRODUCTION

Free energy (FE) calculations are computational physics-based methods that have found numerous applications in fields such as drug discovery,[1−5] where they are widely used in hit finding and lead optimization,[6] and material science.[7−11] Their success is due to their ability to compute free energy differences between thermodynamic states, which ultimately allow scientists to estimate the feasibility of many natural processes such as solvation, protein−ligand binding, and polymerization. In any FE study, the preparation of the system and the analysis of the performed calculations require great attention, and while for the latter, well-established best practices exist,[12,13] it is still not completely clear the effect that the system's preparation has on downstream calculations.

A key part of FE calculations are molecular dynamics (MD) simulations. These are commonly performed with classical force fields (FF), which, in turn, rely on complex parametrization procedures. Van der Waals Lennard-Jones parameters, for example, have been shown to strongly impact hydration free energy calculations.[14] Considerable interest has also been shown in the parametrization of electrostatic interactions, usually described by Coulomb potentials by means of atomic partial charges. Previous studies have shown that solvation free energies are highly sensitive to the parametrization of the solute charges, both in the choice of the charge scheme[15−18] and in the input conformation used to generate the charges.[19,20] These works demonstrate that even small differences in assigned charges can lead to large variations in the computed energies, ultimately compromising the reproducibility and accuracy of the FE calculations. Recently, the MACE-OFF machine learning force field (MLFF)[21−23] has been used to perform hydration free energy calculations of 36 compounds of the FreeSolv data set[24] with great accuracy (root mean squared error of 0.80 kcal/mol). However, the combination of MLFFs with alchemical transformations, while promising, is still in its infancy, and remains more computationally demanding and less established in terms of standardized workflows and sampling efficiency than classical force fields. It is worth to notice that in recent years a plethora of methods to compute solvation free energies have been proposed that completely circumvent alchemical transformations using machine learning (ML) models.[25−30] Although many of those methods report mean absolute errors (MAE) very close to

Received: December 15, 2025
Revised: April 8, 2026
Accepted: April 9, 2026
Published: April 20, 2026

https://doi.org/10.1021/acs.jctc.5c02086
J. Chem. Theory Comput. 2026, 22, 4481−4492

experimental errors, the relative scarcity of experimental data limits their extensive validation, thus understanding of their limitations remains limited as well. Indeed, a recently published benchmark study,[31] has shown how popular ML methods for solvation free energy predictions struggle in terms of transferability to large, flexible molecules. Alchemical transformations, on the other hand, have been thoroughly validated during the last decades and have become the *de facto* standard for free energy calculations in drug discovery.

The problem of choosing a set of partial charges, typically atom-centered, arises because they are not quantum mechanical (QM) observables; hence, there is no unique way to assign them, and the method to derive partial charges is usually decided depending on the specific application. In the context of FE calculations, a common choice is to use electrostatic potential (ESP) or restrained electrostatic potential (RESP) charges.[32,33] These are obtained by fitting the electrostatic potential of the molecule, usually obtained via Hartree−Fock (HF) calculations, within a shell around its van der Waals (vdW) surface. The RESP fitting considers additional restraints aimed at avoiding overpolarization and reducing conformational dependence. Since these charges rely on QM calculations, they are more accurate compared to empirical descriptors but computationally expensive; for this reason, semiempirical methods are generally more popular, especially when needed for high-throughput workflows. The most widely used semiempirical method is AM1-BCC,[34,35] which performs an initial AM1 population analysis[36] and subsequently applies Bond Charge Corrections (BCC) to reproduce RESP charges. This approach inevitably renounces some of the accuracy of first-principle calculations but speeds up the charge assignment, making it possible to parametrize a large number of molecules in a reasonable amount of time (seconds to minutes per molecule, on a single CPU).

To overcome the computational cost of QM calculations, graph and convolutional neural networks have been used to predict high quality charges[37,38] and AM1-BCC charges.[39] For the same scope, simpler architectures employing XGBoost[40] regression and Atom-Path-Descriptors have also been tested.[41] Although all of these studies achieved good predictions on the respective evaluation sets, the effects of their predictions on downstream calculations have not been studied. More oriented to applications to MD simulations was the work of Plé et al.,[42] where the Allegro architecture[43] was used to generate embeddings that were in turn used as input to multilayer perceptrons (MLP) to predict Coulomb and dispersion interaction terms to insert into a classical FF. Here, the Allegro module was trained to get the descriptors and the output of the MLP was a set of pairwise Coulomb contributions, which were used to construct atomic charges. Although charges constructed in this way are useable within their proposed force-field formulation, they are obtained indirectly from learned pairwise interaction decompositions rather than by fitting to the quantum-mechanical electrostatic potential. Consequently, they are not directly comparable to ESP/RESP charges, which are specifically fit to the QM ESP (with regularization in RESP) and are widely validated for transferability and consistency with standard classical force fields (e.g., GAFF).[44] Another challenge in using QM derived charges in fixed charge classical FFs is their dependence on the input conformation. To address this issue, conformational ensemble approaches have been proposed.[45,46] These approaches rely on Boltzmann averages, thus reducing the charge fluctuation within conformations; however, in doing so, they miss the charge enrichment in mutually polarized environments (e.g., water-solute systems) unless conformations are explicitly derived in those environments.

In this work, we tackle the trade-off between accuracy of partial charges and speed of their assignment, and analyze the effect that it has on absolute hydration free energy (AHFE) calculations. To do this, we first use a subset of the FreeSolv data set[24] to prove that calculations initialized with ESP charges are more accurate than those initialized with AM1-BCC charges, both in terms of root mean squared error (RMSE) and ranking (Kendall's τ and Spearman's ρ). The analysis of computed energies and functional groups in the respective molecules draws a nontrivial connection between the quality of the charge assignment and the quality of downstream free energy calculations. We then proceed to propose an ML method for a fast and accurate assignment of ESP charges at a high-fidelity DFT level, employing XGBoost in combination with the pretrained MACE-OFF23(L)[23] force field. This model requires minimal training and in a fraction of a second predicts charges that lead to energies that reproduce the ones obtained with DFT-ESP charges. Finally, we exploit the speed and accuracy of the trained model to propose the Boltzmann Percentile (BP) method to assign ESP-derived charges that are representative of the molecular conformational ensemble in the gas-phase, but favor larger charges in order to approximate polarization effects. On a final set of 30 molecules extracted from the same data set, we show how the BP charges improve AHFE calculations of molecules characterized by conformational flexibility and polar functional groups, with respect to charges predicted on one conformation (in the following referred to as "1-shot charges"), and how both methods perform better than AM1-BCC charges.

METHODS

Computation of Partial Charges

In this work, three methods for computing partial charges are used. The baseline is given by electrostatic potential (ESP) charges, which are obtained by fitting partial charges from a classical Coulomb potential to the quantum-mechanical (QM) molecular electrostatic potential (MESP). This fit is performed using the Merz−Kollman (MK) scheme,[47,48] which performs least-squares optimization to minimize the difference between these two potentials on a set of grid points in van der Waals (vdW) shells around the molecule. This approach can generate sensibly different charges for different input conformations, and is prone to overpolarizing atoms. To avoid these problems, restrained ESP (RESP)[32,33] charges are often used, which perform the fitting procedure with hyperbolic restraints. Both ESP and RESP charges require the computation of the MESP, and this involves expensive QM calculations, often performed with density functional theory (DFT) methods. Semiempirical methods aim to assign partial charges with a reduced computational cost compared to DFT. We focus on AM1-BCC charges,[34,35] which are the most commonly used for free energy calculations. This approach combines AM1 population analysis[36] with Bond Charge Corrections (BCCs), which are aimed at reproducing RESP charges at the Hartree−Fock (HF) level of theory. These charges usually provide a good balance between speed and accuracy and, for this reason, are the common choice when simulating large systems or in high-throughput screening, when the charge assignment has to be performed on a large number of molecules.

ESP charges have been generated using Gaussian16[49] on the self-consistent density (SCF) calculated at the PBE0 level of theory,[50,51] with def2-TZVP[52,53] basis set and the D3 version of Grimme's dispersion with Becke-Johnson damping (GD3BJ).[54] RESP charges were calculated by first computing the SCF and ESP charges at the HF/6-31G* level of theory,[55,56] and then extracted using the Antechamber function of the AmberTools module.[57] Finally, AM1-BCC charges were assigned through the AmberTools Toolkit Wrapper of OpenFF.[58,59]

https://doi.org/10.1021/acs.jctc.5c02086
J. Chem. Theory Comput. 2026, 22, 4481−4492

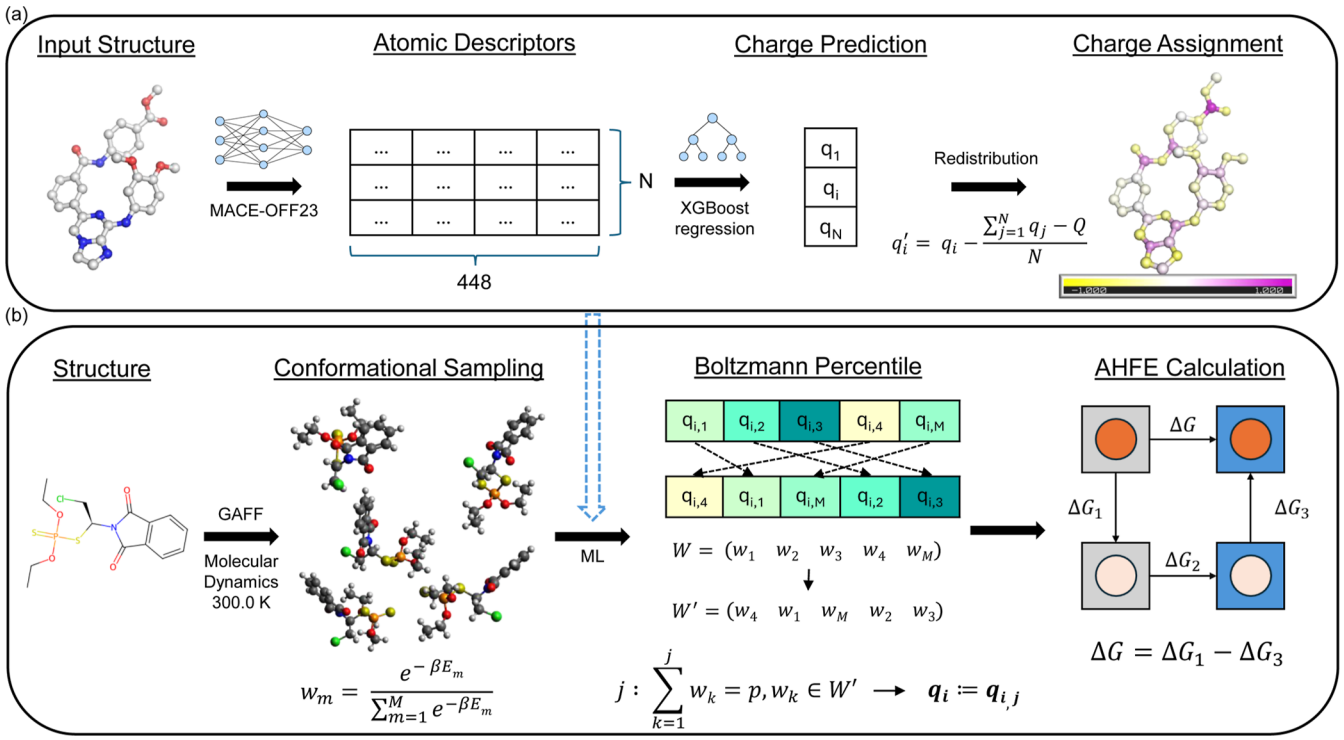

Figure 1. (a) Architecture of the model. MACE-OFF is used to generate atomic embeddings that are fed as input to an XGBoost algorithm, which ultimately predicts charges. (b) Boltzmann Percentile method. MD is performed on the input structure to sample conformations. Charges predicted on each conformation are then combined with Boltzmann weights to favor large charges from conformations with high probability.

Prediction of Partial Charges

Figure 1a shows the design of the ML model used to predict partial charges. The model takes as input atomic numbers and coordinates and uses the pretrained MACE-OFF force field in the 23(L) version[23] to generate atomic descriptors. These descriptors are, in turn, used as input for an XGBoost regression algorithm[40] that predicts atomic charges. Charges predicted in this way are not restrained to conserve total charge, so before assignment, an additional step is performed to distribute the difference between the sum of predicted partial charges and the total charge of the molecule evenly among all atoms. The XGBoost model was trained on gas-phase structures from the Aquamarine (AQM) data set,[60] which contains a total of 59,783 conformations from 1653 unique drug-like molecules, with sizes ranging from 2 to 92 atoms, and containing an average of 28.2 non-hydrogen atoms belonging to elements C, N, O, F, P, S, and Cl. For each structure, a MACE descriptor was generated with the ASE package,[61] and ESP charges were computed as described above. 70% of the data set was used for training, 20% for validation, and 10% for testing. Optimization was performed with Optuna.[62]

Boltzmann Percentile

To estimate representative values of atomic ESP charges from an ensemble of conformations, we introduce a Boltzmann-weighted percentile approach (BP), as depicted in Figure 1b. Consider a molecule with N atoms and an ensemble of M conformations. Each conformation m is characterized by its energy E_m and the vector of atomic charges

$$\mathbf{Q}_m = (q_{1,m}, q_{2,m}, ..., q_{N,m})$$

Each conformation is assigned a normalized Boltzmann weight

$$w_m = \frac{e^{-\beta E_m}}{\sum_{m=1}^{M} e^{-\beta E_m}}$$

where $\beta = 1/(k_B T)$. For each atom i, the set of charge values $\{q_{i,1}, q_{i,2}, ..., q_{i,M}\}$ defines a Boltzmann-weighted distribution. These values are first sorted in ascending order (in magnitude), and the corresponding cumulative distribution is computed as

$$C_i(q_{i,j}) = \sum_{k:q_{i,k} \le q_{i,j}} w_k$$

The Boltzmann-weighted p-th percentile charge of atom i, denoted $q_{i,p}$, is then defined as the smallest charge value satisfying

$$C_i(q_{i,p}) \ge p, \quad p \in [0, 1]$$

For example, p = 0.90 corresponds to the 90th percentile of the Boltzmann weighted charge distribution for atom i.

This procedure is applied independently to each atom, yielding a set of representative charges $\{q_{i,p}\}_{i=1}^{N}$ that reflect both the thermodynamic probabilities of the sampled conformations and the tail behavior of each atomic charge distribution. After charges are assigned to each atom, the total charge surplus (or deficit) is redistributed as previously discussed. The BP estimator thus provides an alternative to the traditional Boltzmann-weighted average, emphasizing statistically significant extreme values rather than mean behavior. This choice is justified by the fact that solute and water mutually polarize each other, leading to larger charges. A simple averaging suppresses extreme values and, as a consequence, FE calculations tend to overestimate AHFEs, as shown in Figure S1a of the Supporting Information.

To sample conformations and compute energies, we performed molecular dynamics (MD) simulations in gas-phase using the OpenMM simulation package.[63] The systems were parametrized using the GAFF force field[44] (for consistency with the parametrization of the following AHFE calculations) and equilibrated under Langevin dynamics at a temperature of 300 K with a friction coefficient of 1 ps^{-1}. A time step of 2.0 fs was employed for the numerical integration of the equations of motion. Following energy minimization, a 1 ns production simulation was carried out, which we considered a good compromise for sampling conformations while maintaining rapid parametrization. Atomic coordinates were saved every 1000 integration steps (equivalent to 2 ps per frame), resulting in a total of 500 trajectory

https://doi.org/10.1021/acs.jctc.5c02086
J. Chem. Theory Comput. 2026, 22, 4481−4492

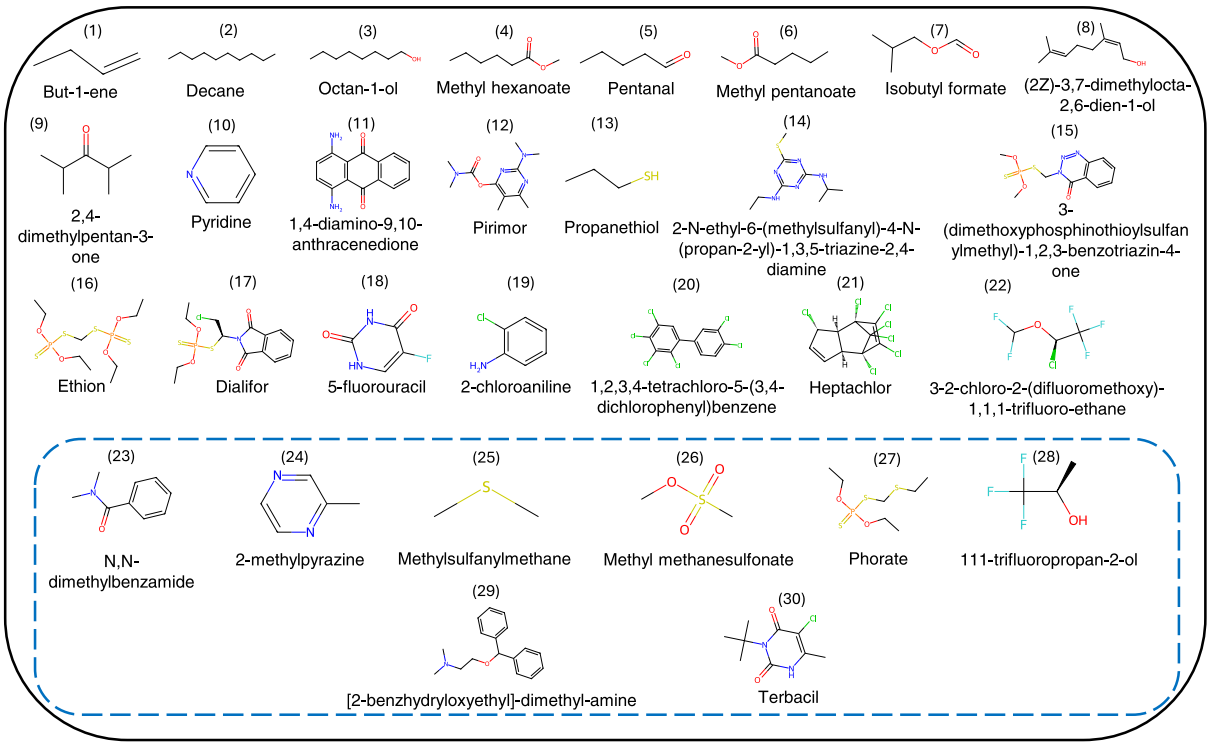

Figure 2. Systems selected for AHFE calculations. The blue box indicates the 8 extra molecules selected for the final assessment. The number in parentheses above each molecule is an index added for easy identification in the following parity plots.

frames, on which charges were predicted with the previously presented ML model, and the 90-th percentile was used for the assignment.

Compound Selection and Analysis

The compounds studied in this work were selected from the FreeSolv data set,[24] which contains experimental hydration free energies for 643 molecules. We initially selected 22 molecules with typical moieties found in drug-like molecules, to which we added 8 more molecules containing polar functional groups for the final assessment. Figure 2 shows the selected molecules with names as reported in FreeSolv and 2D images drawn with RDKit.[64] The selected molecules are small to medium size, with a minimum size of 11 atoms, a maximum of 41, and a mean of 23.81. The selection also spans different types of chemistry, from simple, small organic compounds to more complex aromatic heterocycles, organosulfurs, and halogenated compounds.

To connect the accuracy of the AHFE calculations with the presence of certain functional groups, we computed the total charge assigned to each group with three different assignment methods (ESP, AM1-BCC, and BP). The functional groups for each molecule are stored in the FreeSolv data set and the specific atoms belonging to a group were found with RDKit's `GetSubstructMatches`. The total charge assigned by each method to each group, as well as the occurrence of each group, are shown in Figure 6.

To compare the sensitivity of different charge assignments to the input conformation, we studied the change in atomic charges across different conformers of flexible molecules. For the sake of this analysis, we define molecules as flexible when the root mean squared deviation (rmsd) of the original structure in the input file from the geometry after geometry optimization with the UFF force field[65] (on which charges are assigned) exceeded 2Å. In the set of 22 molecules, only 6 met this criterion, of which 4 were selected as test cases for the analysis: 3-(dimethoxyphosphinothioylsulfanylmethyl)-1,2,3-benzotriazin-4-one (RMSD = 2.39 Å), dialifor (2.99 Å), ethion (4.00 Å), and (2Z)-3,7-dimethylocta-2,6-dien-1-ol (2.51 Å). For each of these molecules, we generated nine distinct conformers with RDKit's `EmbedMultipleConfs` method. The RDKit's conformer generation procedure differs from the conformational sampling employed by the BP model, in that it follows a distance geometry approach instead of a dynamical one. The interested reader can find a plot of the structural difference between the 9 conformers for each molecule in the Supporting Information (Figure S2).For each of the 9 conformers we assigned charges with ESP, RESP, and BP as described above and constructed bar plots of the standard deviation of the atomic charges for each charging scheme (Figure 4). The choice of adopting a different structure generation scheme than the one employed for the BP charge assignment, which involved larger structure ensembles with strongly correlated conformations, ensured a more straightforward comparison of the conformational dependence of partial charges derived with the three different approaches.

Free Energy Calculations

We have performed free energy calculations with the same exact settings but five different parametrizations of the solute's charge assignment: AM1-BCC (semiempirical), ESP (from QM calculations), RESP (from QM calculations), 1-shot (ML-derived on the input conformation), and BP (ML-derived on the conformational ensemble). All absolute hydration free energy (AHFE) calculations were performed using the `AbsoluteSolvationProtocol` of the OpenFE package.[66] This protocol performs an alchemical transformation by annihilating the solute's Coulombic interactions and subsequently decoupling its Lennard–Jones interactions from the solvent environment. Each transformation was sampled over 22 λ-windows, and four independent protocol repeats were executed to improve statistical reliability. The solute parameters were generated using the GAFF force field,[44] and the systems were solvated in explicit TIP3P water[67] with a cubic box and a solvent padding of 1.5 nm. Simulations were conducted at 298.15 K and 1 atm using a Langevin thermostat (collision rate 1 ps^{-1}) and a Monte Carlo barostat applied every 25 integration steps. A time step of 4 fs was employed with all bonds involving hydrogen atoms constrained, and the masses of hydrogen atoms increased. Nonbonded interactions were treated using the particle mesh Ewald (PME) method[68] with a real-space cutoff of 1.0 nm. For each λ-state, production simulations were run for 10 ns in solvent and 2 ns in vacuum, following energy minimization and equilibration phases. Free energy estimates were obtained from the multistate Bennett acceptance ratio (MBAR)[69] analysis as imple-

https://doi.org/10.1021/acs.jctc.5c02086
J. Chem. Theory Comput. 2026, 22, 4481−4492

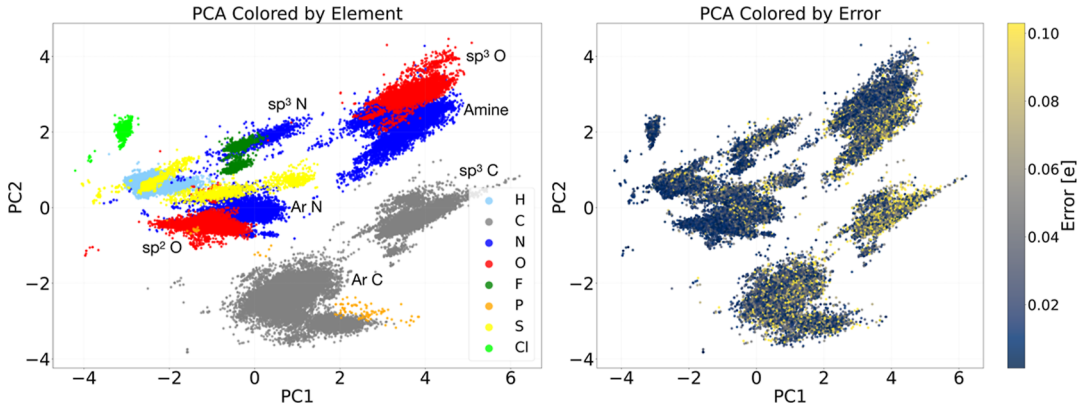

Figure 3. (left) 2D PCA projection of atomic descriptors colored by element. C, N, and O can be found in different distinct clusters, according to the atom type (as provided by OpenBabel). Carbon can be found in sp^3 hybridization and in Aromatic (Ar) form, while Oxygen in sp^3 and sp^2 hybridizations. N can be found in three different forms: Aromatic, Amine, and hybridized sp^3. (right) Same projection but colored by prediction error.

Table 1. Root Mean Squared Error for the Most Common Atom Types in the Test Set, as Reported by OpenBabel

	H	Ar C	sp^3 C	Amine	sp^3 N	Ar N	sp^3 O	sp^2 O	F	P	S	Cl
RMSE [e]	0.02	0.06	0.09	0.08	0.07	0.05	0.03	0.02	0.01	0.05	0.05	0.01

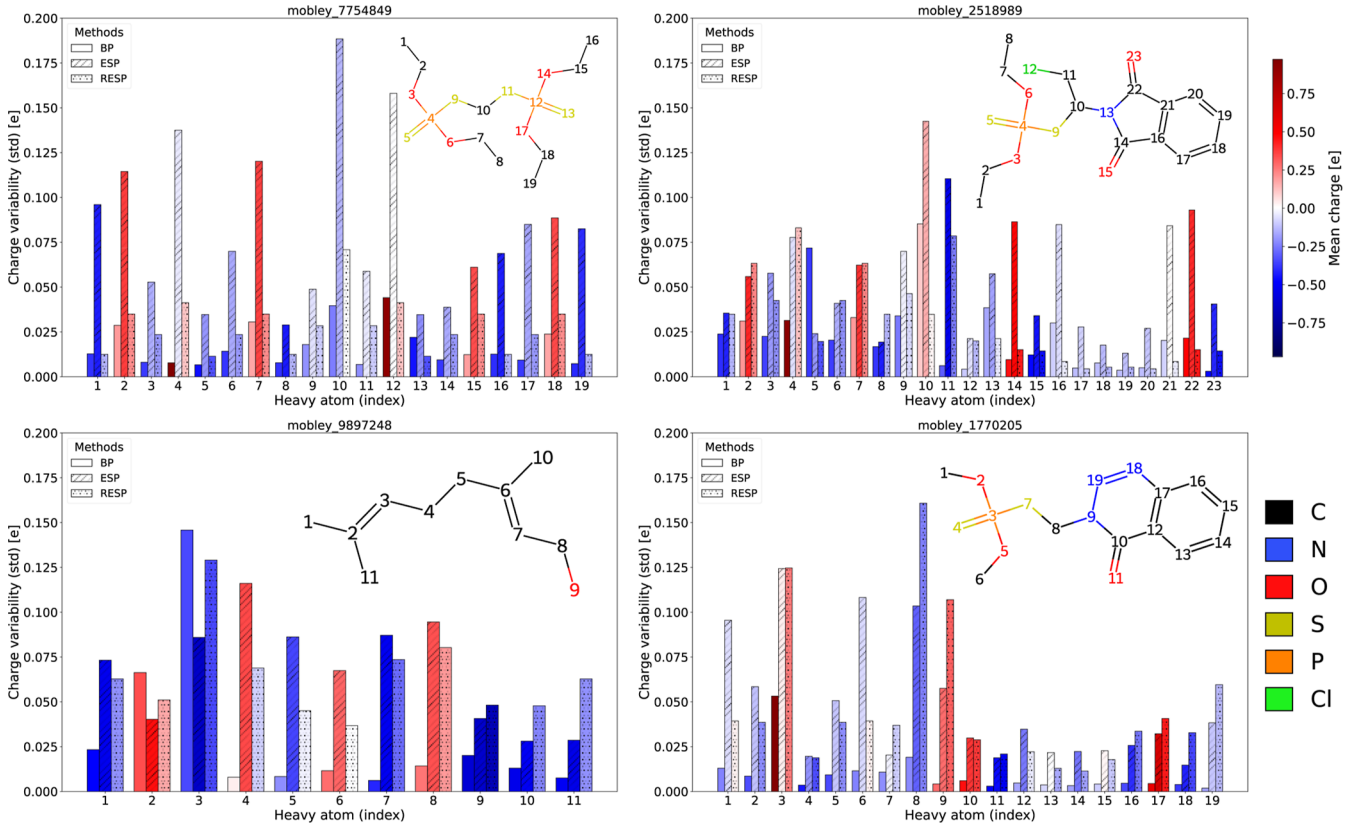

Figure 4. Variability of atomic charges for 9 different conformers for BP, ESP, and RESP method. The height of the bar indicates the standard deviation of the assigned charge, while the color indicates the mean value.

mented in OpenFE. All nonmentioned settings were maintained at their OpenFE defaults.

RESULTS AND DISCUSSION

Model Validation

The root mean squared error on the test set, composed of 10% of AQM (around 300,000 atoms) was 0.05 e, indicating a generally good prediction. The accuracy of the predictions is not the same for all atomic species, which is deducible from Figure 3. The left panel of the figure shows a two-dimensional principal component analysis (PCA)[70] of the atomic descriptors, colored by element. The MACE descriptors effectively group different elements in different regions of the latent space. Moreover, different atomic species (reported as OpenBabel[71] atom types) of the same element are also grouped separately. Interestingly, the proximity of different species is chemically reasonable. For

https://doi.org/10.1021/acs.jctc.5c02086
J. Chem. Theory Comput. 2026, 22, 4481−4492

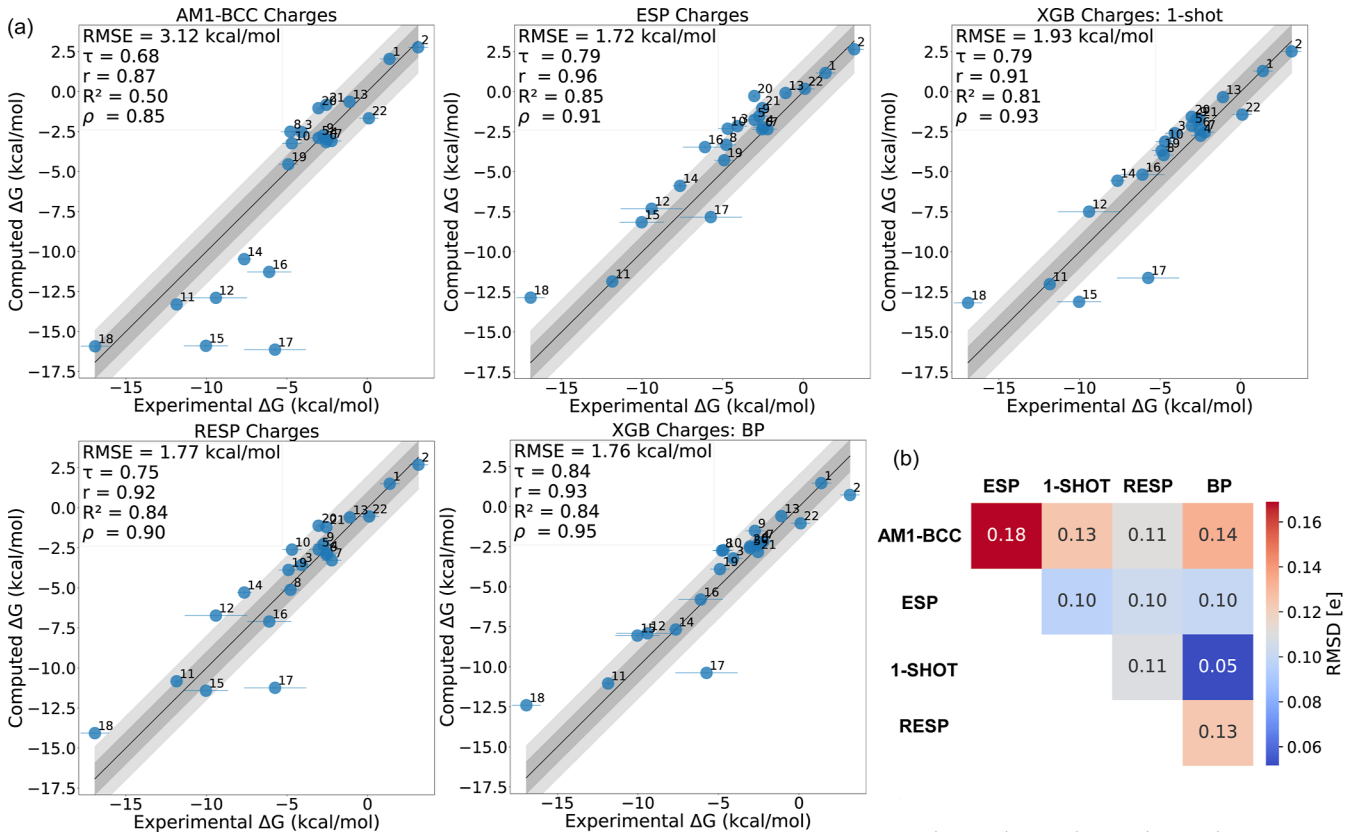

Figure 5. (a) Calculated versus experimental hydration free energies for the five charge assignment methods. Plots report root mean squared error, Kendall's τ, Pearson's correlation coefficient r, R^2 score, and Spearman's ρ. Each point reports the molecular index as defined in Figure 2 for easy reference. (b) Pairwise root mean squared deviation of assigned charges for the 22 considered molecules.

example, amine N and sp^3 O are very close in the reduced space, and indeed they are both heteroatoms with lone pairs in sp^3 hybrid orbitals, typically bonded to carbon and hydrogen. So, they have comparable local geometries (roughly tetrahedral), and this is what is captured by the employed geometric descriptors.

The right panel of Figure 3 shows the same bidimensional projection but colored by absolute prediction error. It appears clear that C and N, which have the largest number of different bonding patterns they can participate in, are the elements with larger prediction errors, while H, O, F, and Cl show very small errors. Instead, P and S are predicted with an accuracy in between the two (0.05 e). In terms of accuracy on different atomic types of the same element, charges on aromatic C and N atoms are slightly more accurate than on the same elements in hybridization sp^3 (Table 1). This analysis suggests that there are two main factors that determine the prediction error: a large variety of bonding patterns (C and N) and small occurrence of atoms in the training data (P, S). Ulterior studies may aim at improving predictions on these elements, but as shown in the following, the current accuracy is enough to have significant improvements on AHFE calculations.

In order to elevate the evaluation from an atom-wise perspective to the molecular level, it is necessary to look at the effects that the charge redistribution step has on the final charge assignment. On the 30 molecules from FreeSolv analyzed in the following, the magnitude of the molecular charge before correction deviates on average by 0.16 e from the correct one, which is zero for all molecules. The magnitude of the average atomic correction is 0.008 e. Although this value is largely below the accuracy of the model discussed above, enforcing the correct total charge is an essential step to avoid systematic, method-dependent artifacts. Under PME with periodic boundary conditions, in fact, AHFEs of charge solutes are sensitive to the net charge and its interactions with the neutralizing background.[72] Importantly, for the analyzed molecules, the correction does not cause relevant sign changes that could significantly impact electrostatic interactions between an atom and the environment, and potentially affect the AHFE calculation.

Conformational Dependence of Molecular Charge Distribution

The sensitivity of AHFE calculations to different charge assignments found in previous works[15,16,19,20] means that methods with strong conformational dependence, such as ESP, struggle in terms of reproducibility and, if the starting conformation is unrealistic, accuracy. The necessity of robustly assigning charges with different input conformations is one of the reasons RESP charges were introduced. The BP method also reduces the conformational sensitivity of ESP charges and, in the majority of cases, the assigned charges are even less variable than RESP ones. Figure 4 shows the charge variation for each compound atom across nine conformations, for four flexible compounds. As expected, the restraints in the fitting procedure ensure that RESP charges are less variable than ESP charges, i.e. charges assigned to the same atoms of the same molecule tend to be more similar across different conformations. BP assignment not only replicates this result, but the corresponding charge distributions are even narrower than for RESP charges in most cases. This shows that for the large majority of compound atoms,

https://doi.org/10.1021/acs.jctc.5c02086
J. Chem. Theory Comput. 2026, 22, 4481−4492

the proposed method assigns charges that are less conformation-dependent than those of the well-assessed RESP method. The robustness of BP comes from using an ensemble method, which avoids structure initialization bias, when starting with an unsuitable conformation. So, rather than assigning charges to a single, possibly unrealistic, structure, the method considers several likely states.

The coloring in Figure 4 also suggests that atomic charges averaged across conformations are qualitatively similar within the three methods. A notable exception are phosphate atoms, for which BP assigns larger charges than the (R)ESP reference method. Despite this localized difference, the increased polarization does not translate into a significant deterioration of the computed hydration free energies within the present data set. The only molecules in the selection that contain P atoms are 3-(dimethoxyphosphinothioylsulfanylmethyl)-1,2,3-benzotriazin-4-one, *ethion*, and *dialifor*. In the next section, we discuss how BP charges lead to more accurate AHFE for these compounds compared to AM1-BCC charges.

In brief, the Boltzmann percentile method generally assigns charges that maintain the environmental awareness and the quality of ESP charges but are less dependent on the input conformation than RESP charges and thus promise to improve AHFEs and likely free energy calculations in general with respect to traditional charge assignment methods. The proposed method should be interpreted as an effective ensemble-based parametrization that enhances the magnitude of electrostatic features relevant in solute−solvent interactions, rather than as a model intended to reproduce a physical electronic distribution. In fact, due to the charge selection procedure, the final charge vector may combine values originating from different conformations and does not necessarily preserve the full joint covariance structure of correlated charge fluctuations (e.g., local charge compensation between neighboring atoms). This was confirmed on a test based on the Mahalonobis distance[73] between BP assigned charges and the sampled charge distributions of the 30 selected molecules. The interested reader can find the analysis in the "Charge Correlation" section in the Supporting Information. While such correlation breaking could be consequential in applications requiring electrostatic realism or accurate polarization fluctuations, the following results demonstrate that preserving the exact joint distribution is not a prerequisite for improving solvation free energies in water.

Effect of Different Partial Charge Assignment Methods on AHFEs

Figure 5a shows, for the 22 molecules in Figure 2, the experimental AHFEs versus those computed from AM1-BCC, ESP, 1-shot, RESP, and BP charges. The plots also report RMSE, Kendall's τ, Pearson's r, explained variance R^2, and Spearman's ρ. These metrics are also reported in Table 2. The highest RMSE, 3.12 kcal/mol, is obtained with AM1-BCC charges and is significantly higher than the average RMSE reported on the entire FreeSolv data set (1.51 kcal/mol). This is due to the particular selection of compounds, which is meant to analyze the ability of the proposed method to improve traditional calculations where they are known to struggle. The average RMSE reported for the same subset of molecules in the original publication coincides with the one obtained by our calculations. This consistency validates the calculations settings used. The lowest RMSE, 1.72 kcal/mol, is obtained with ESP charges and is considerably closer to the mean experimental error of the references (0.71 kcal/mol). ML-predicted charges from one conformation replicate this result fairly well, only slightly increasing the error (1.93 kcal/mol). The RESP and BP charges, instead, lead to an almost identical error (1.77 and 1.76 kcal/mol respectively). This is in slight contrast with a previous study which found that RESP charges applied to GAAMP reparameterization of GAFF lead to worse AHFEs predictions than GAFF with AM1-BCC charges.[74] These results were obtained on different systems, so it is not trivial to determine whether the tension stems from the FF parametrization or the systems selection.

Table 2. Root Mean Squared Error, Kendall's τ, Pearson's Correlation Coefficient r, Explained Variance R^2, and Spearman's ρ of Calculated Values of AHFE for 22 Molecules of the FreeSolv Dataset with Different Charge Assignments

	RMSE [kcal/mol]	τ	r	R^2	ρ
AM1-BCC	3.12	0.68	0.87	0.50	0.85
ESP	**1.72**	0.79	**0.96**	**0.85**	0.91
XGB: 1-SHOT	1.93	0.79	0.91	0.81	0.93
RESP	1.77	0.75	0.92	0.84	0.90
XGB: BP	1.76	**0.84**	0.93	0.84	**0.95**

In addition to the RMSE, ranking performances also improve when using ESP instead of AM1-BCC, with Kendall's τ increasing from 0.68 to 0.79 and Spearman's ρ from 0.85 to 0.91. Approximately the same ranking scores are obtained with the 1-shot charge assignment, while the best are obtained with BP charges (τ = 0.84, ρ = 0.95).

The differences in free energies calculated from ESP and from AM1-BCC charges somehow reflect the differences between the charges themselves. In fact, as shown in Figure 5b, the average root mean squared deviation between charges assigned with these two methods is large (0.18 e). However, there is no clear way to predict a priori how changes in partial charges will affect the resulting AHFE results. For example, the row corresponding to ESP in Figure 5b shows that 1-shot, RESP, and BP charging methods also have non-negligible differences (0.10 e); nevertheless, RMSEs of calculated energies are similar. A reason for this could be that these methods, while globally assigning charges rather different from ESP, assign similar charges on the atoms that actively lead the dynamics, i.e. on some important functional groups. Figure 6 reports a min/max plot of the total charge assigned to the various functional groups of the selected molecules by ESP, AM1-BCC, and BP. The name of the group is followed by a number in parentheses indicating the number of occurrences of that group in the selection. For many groups, the mean values obtained with the three methods are similar, but for some AM1-BCC assign a total charge that is radically different from the other methods. It is possible to connect these groups with the outliers of the AHFE calculations reported in Figure 5a (defined as having an absolute error larger than 2.00 kcal/mol).

The poor results of calculations with AM1-BCC charges are mainly imputable to 5 outliers, corresponding to indices 14, 16, 12, 15, 17. These correspond in order to 2-*N*-ethyl-6-(methylsulfanyl)-4-N-(propan-2-yl)-1,3,5-triazine-2,4-diamine, *ethion*, *pirimor*, 3-(dimethoxyphosphinothioylsulfanylmethyl)-1,2,3-benzotriazin-4-one, and *dialifor* (Figure 2). 2-*N*-ethyl-6-(methylsulfanyl)-4-*N*-(propan-2-yl)-1,3,5-triazine-2,4-diamine is the only molecule reporting secondary amine and secondary aromatic amine groups. For both these groups, the total charge assigned to the group by AM1-BCC is notably different from the charges assigned by ESP and BP. The absolute error obtained

https://doi.org/10.1021/acs.jctc.5c02086
J. Chem. Theory Comput. 2026, 22, 4481−4492

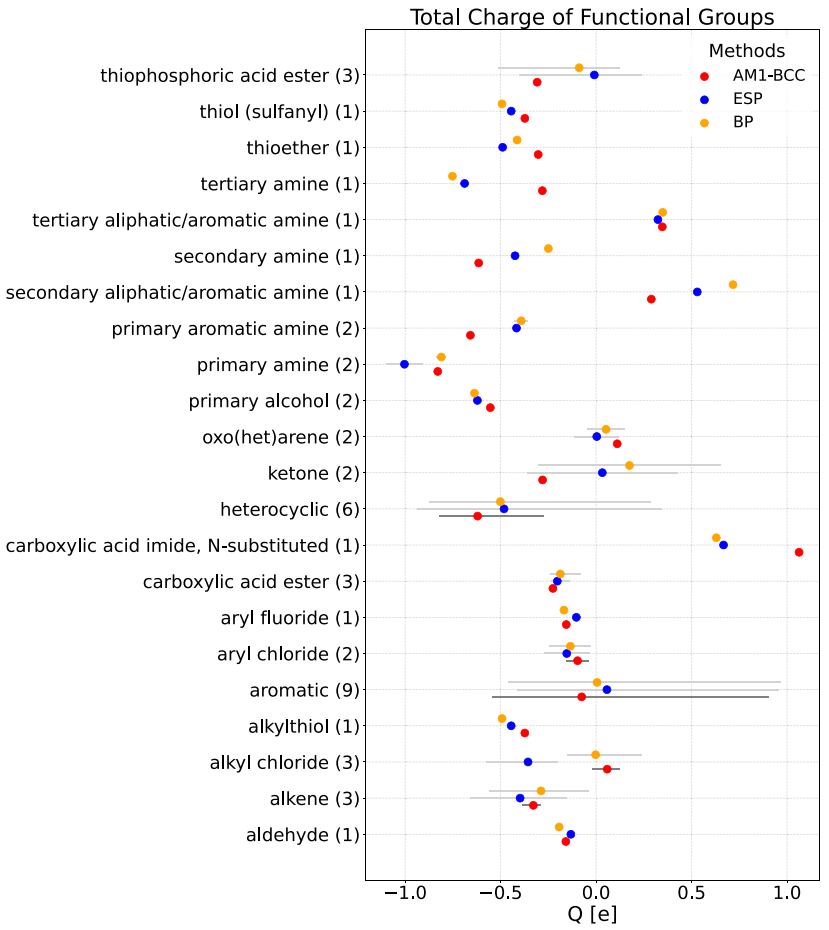

Figure 6. Total charge on functional groups of the 22 selected molecules of the FreeSolv data set, as assigned by ESP, AM1-BCC, and the BP method. The number in parentheses refers to the occurrence of the group. The points indicate the mean value, and the bars range from the minimum to the maximum value.

using semiempirical charges is 2.83 kcal/mol, and reduces to 1.77 kcal/mol with ESP charges (0.02 kcal/mol with BP).

Ethion contains thiophosphoric acid ester. This group also belongs to two other outliers: 3-(dimethoxyphosphinothioylsulfanylmethyl)-1,2,3-benzotriazin-4-one and *dialifor*. Like the secondary amine groups, for this group, the AM1-BCC charges differ largely from the ESP and BP charges. Moreover, these two methods show a variability in charge due to different environments that the AM1-BCC method neglects. This unawareness of the local environment is directly reflected in AHFE calculations: *ethion* misestimates the experimental value by 5.18 kcal/mol when calculated with semiempirical charges and by 2.64 kcal/mol with ESP charges (0.30 kcal/mol with BP). The other two molecules containing this group also get lower errors when using ESP (BP) charges: 3-(dimethoxyphosphinothioylsulfanylmethyl)-1,2,3-benzotriazin-4-one from 5.87 to 1.88 kcal/mol (1.98 kcal/mol with BP), *dialifor* from 10.40 to 2.09 kcal/mol (4.64 kcal/mol with BP). All of these molecules contain hypervalent phosphorus/sulfur, on which the BCC corrections were not trained extensively and have already been shown to perform poorly.[75]

Dialifor contains other two functional groups for which AM1-BCC and ESP charges differ significantly: carboxylic acid imide, *N*-subsistuted, and alkyl chloride. The first is present only in this molecule, while the second is also present in 3-2-chloro-2-(difluoromethoxy)-1,1,1-trifluoro-ethane and *heptachlor*. These two molecules are not outliers for calculations with AM1-BCC charges, but it is interesting to note that calculations with ESP charges still show lower errors: from 1.77 to 0.08 kcal/mol for the former and from 1.72 to 1.52 kcal/mol for the latter. For this group BP charges show values more similar to AM1-BCC than ESP, nevertheless they still lead to lower errors: 1.14 kcal/mol for 3−-2-chloro-2-(difluoromethoxy)-1,1,1-trifluoro-ethane and 0.28 kcal/mol for *heptachlor*.

Finally, *pirimor* contains tertiary amine, on which a previous study found calculations with AM1-BCC charges more accurate than with RESP charges.[76] For this molecule, the error actually reduces from 3.49 to 1.91 kcal/mol (1.50 kcal/mol) when using ESP (BP) charges instead of AM1-BCC. However, a larger number of compounds with tertiary amines would be needed for a more thorough comparison in this case.

The previous analysis showed that, as expected, ESP charges can better capture the chemical environment of molecules than semiempirical charges, and when the charges assigned with the two methods are significantly different, calculations with QM charges are always more accurate. Interestingly, these cases correspond exactly to the cases in which AM1-BCC is known to struggle: heavily halogenated alkanes, polar compounds, and hypervalent phosphorus/sulfur. The comparison with BP charges showed that even though the difference in charges may be large on the whole molecule, the Boltzmann Percentile method assigns charges that are compatible with DFT-derived charges on the relevant functional groups, and this results in similar AHFEs. Nevertheless, the accuracy of the underlying ML

https://doi.org/10.1021/acs.jctc.5c02086
J. Chem. Theory Comput. 2026, 22, 4481−4492

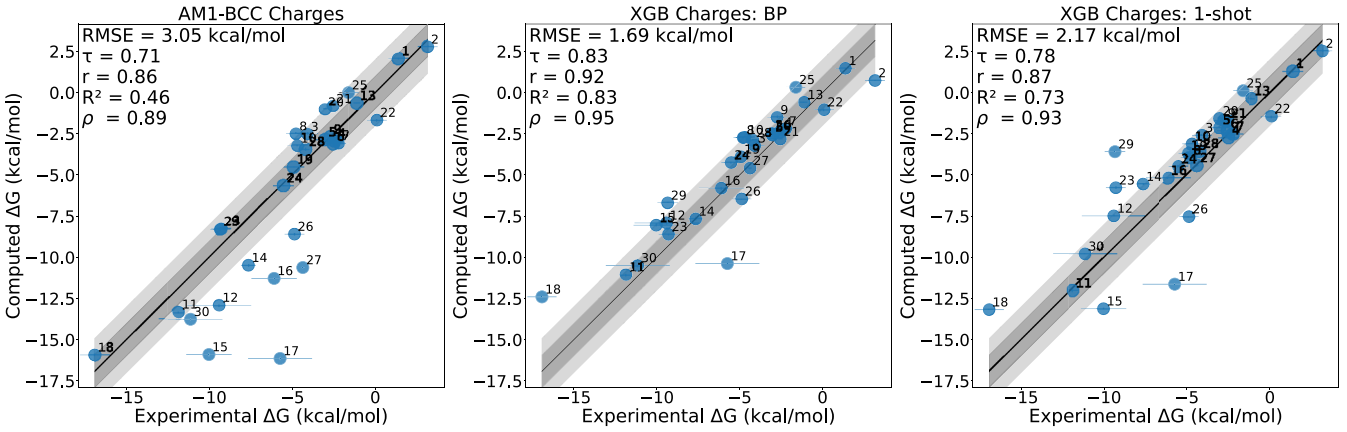

Figure 7. Parity plots of computed versus experimental AHFEs for the extended set of 30 molecules, with charges assigned with the AM1-BCC, 1-shot, and BP methods.

model seems to be the greatest limitation to the BP model. An example of this limitation is the previously mentioned *dialifor*, which is the only molecule of those mentioned in the previous analysis, for which the energy computed from BP charges is substantially worse than the energy computed with ESP charges. The RMSD of 1-shot and ESP charges assigned to this molecule is 0.21 e for the same structure, and the deviation from the experimental AHFE calculated with these charges is 5.89 kcal/mol. The BP method, due to its ensemble-based nature, reduces this error by 1.30 kcal/mol but cannot overcome the intrinsic inaccuracy of the charges, thus yielding an error which is still approximately 2.50 kcal/mol larger than that obtained with ESP charges. This demonstrates the importance of an accurate description of the molecular charge distribution for deriving reliable AHFEs, especially in the presence of functional groups that are polar, form strong hydrogen bonds, or contain moieties that were underrepresented in the fitting of BCC corrections. Our ML model provides a sufficiently accurate electrostatic description in the majority of these cases in a fraction of a second, which is negligible with respect to DFT calculations and even shorter than AM1-BCC assignment (Table S1 in Supporting Information).

AHFE on Extended Set of Test Molecules

The previous analysis showed that the difficulty for semiempirical methods to assign charges on certain moieties directly results in poor AHFE calculations. However, in the previous selection of molecules, these moieties were not highly represented. To analyze the robustness of different methods to an increased frequency of complex functional groups, we selected eight more molecules (dashed box in Figure 2), and calculated AHFE from AM1-BCC, 1-shot, and BP charge assignments. Figure 7 shows the parity plots for the three methods on the final set of 30 molecules. The final metrics do not change sensibly, except for a slight increase in RMSE for 1-shot charges. Nevertheless, these charges still give more accurate calculations than AM1-BCC. Three of these 8 molecules are outliers for AM1-BCC charges: methylmethanesulfonate, phorate, and terbacil. All of these molecules get good estimates using BP charges, which show only one small outlier: [2-benzhydryloxyethyl]-dimetyhl-amine. The other two outliers for this method were already present in the previous batch of calculations and are *dialifor* and *5-fluorouracil*. Calculations with DFT charges also showed an outlier for *fluorouracil*, indicating that QM calculations have difficulties with this compound, so ML cannot improve its description. [2-benzhydryloxyethyl]-dimetyhl-amine and *dialifor* have in common a double aromatic structure and a large number of rotatable bonds. For these compounds, assigning fixed charges is likely to be problematic. Moreover, better treatment of dispersion interactions is likely to help. The ranking performances also do not change and the BP charges ensure an extremely good ranking (τ = 0.83 and ρ = 0.95). All together, these results, obtained on a more diverse set of molecules, are consistent with our previous findings, further validating our proposed methodology.

CONCLUSIONS

In this work, we highlight the pivotal role of the electrostatic description of molecules when performing alchemical transformations to derive absolute hydration free energies (AHFEs). The traditional approach involves force fields with atomic partial charges assigned through semiempirical methods, typically with the AM1-BCC method, which renounces some of the accuracy of DFT calculations in exchange for a significant speed-up in the parametrization. The underlying assumption of this approach is that the loss stemming from less accurate charges will not drastically affect the results. However, we demonstrated that when the molecules under investigation contain functional groups that are known to be challenging to describe with semiempirical methods, the reliability of free energy calculations is directly compromised, despite of sometimes even relatively small charge changes. To overcome this problem, we propose and make available an ML model, trained on high-fidelity DFT data (PBE0-D3(BJ)/def2-TZVP level) of comprehensive size, to reproduce QM-based ESP charges with small error (0.05 e), at a fraction of their computational cost. The speed of the predictive model also allows us to propose a new method, namely the Boltzmann Percentile method, to assign charges that are representative of the conformational ensemble of the input molecules, thus overcoming the problem of the conformational dependence of ESP charges and avoiding a dependence on a single, potentially nonrepresentative molecular conformation.

The proposed method produces charges that are even less variable than RESP charges, at the minimal extra cost of a short single MD simulation in gas-phase. Even charge prediction based on a single conformation already achieves better agreement with experimentally measured hydration free energies (RMSE = 2.17 kcal/mol) and improves free energy ranking in comparison to calculations involving semiempirical charges (RMSE = 3.05 kcal/mol). The BP method further

https://doi.org/10.1021/acs.jctc.5c02086
J. Chem. Theory Comput. 2026, 22, 4481−4492

enhances these improvements (RMSE = 1.69 kcal/mol). Therefore, we offer a computationally efficient and reliable way to parametrize the electrostatic terms of classical force fields, which adds only a negligible extra cost to traditional workflows and significantly improves AHFE results. Although our approach demonstrated successful for derivation of solvation free energies, which are highly sensitive to parametrization, we remain agnostic on whether to consider our approach as a general correction to GAFF, and leave for future works to validate it on other properties (e.g., enthalpies of vaporization, liquid densities, etc.···). As a further step, suitability of our charge assignment method for ligand binding free energies will be tested. The high computational cost of free energy calculations remains one of the bottlenecks of physics-based computer-aided drug design. Improving the reliability of such calculations without further increasing the computational burden, as demonstrated in this work, will contribute to improving the quality of virtual screening efforts that are routinely used in typical drug discovery projects.

■ ASSOCIATED CONTENT

Data Availability Statement

The data underlying this study are openly available on GitHub at this repository: https://github.com/mathilfiker/ml_for_charges. The training, validation, and test sets are available as a Zenodo repository (https://doi.org/10.5281/zenodo.17790331).

Supporting Information

The Supporting Information is available free of charge at https://pubs.acs.org/doi/10.1021/acs.jctc.5c02086.

Time needed for charge assignment with AM1-BCC, DFT, and XGBoost on each of the 22 molecules, AHFE calculations with Boltzmann Average and Boltzmann 75-percentile, full list of calculated AHFEs with all the charge assignments, rmsd analysis of conformers generated for the conformational flexibility analysis, charge correlation analysis for BP charges (PDF)

■ AUTHOR INFORMATION

Corresponding Author

Marco Klähn − *Molecular AI, Discovery Sciences, Gothenburg 43183, Sweden;* orcid.org/0000-0002-9369-4819; Email: marco.klahn@astrazeneca.com

Authors

Mathias Hilfiker − *Department of Physics and Materials Science, University of Luxembourg, Luxembourg City L-1511, Luxembourg; Molecular AI, Discovery Sciences, Gothenburg 43183, Sweden;* orcid.org/0009-0008-9401-3262

Leonardo Medrano Sandonas − *Institute for Materials Science and Max Bergmann Center for Biomaterials, TUD Dresden University of Technology, Dresden 01062, Germany;* orcid.org/0000-0002-7673-3142

Alexandre Tkatchenko − *Department of Physics and Materials Science, University of Luxembourg, Luxembourg City L-1511, Luxembourg;* orcid.org/0000-0002-1012-4854

Ola Engkvist − *Molecular AI, Discovery Sciences, Gothenburg 43183, Sweden; Department of Computer Science and Engineering, Chalmers University of Technology and University of Gothenburg, Gothenburg 41296, Sweden;* orcid.org/0000-0003-4970-6461

Complete contact information is available at: https://pubs.acs.org/10.1021/acs.jctc.5c02086

Notes

The authors declare no competing financial interest.

■ ACKNOWLEDGMENTS

The study was partially supported by the Marie Sklodowska-Curie Innovative Training Network European Industrial Doctorate grant agreement No. 956832 “Advanced machine learning for Innovative Drug Discovery” (AIDD).

■ REFERENCES

(1) Cournia, Z.; Chipot, C. Applications of free-energy Calculations to Biomolecular Processes. a Collection. *J. Phys. Chem. B* **2024**, *128*, 3299−3301.

(2) Shirts, M. R. Best practices in free energy calculations for drug design. *Computational drug discovery and design* **2012**, *819*, 425−467.

(3) Cournia, Z.; Allen, B.; Sherman, W. Relative binding free energy calculations in drug discovery: recent advances and practical considerations. *J. Chem. Inf. Model.* **2017**, *57*, 2911−2937.

(4) Qian, R.; Xue, J.; Xu, Y.; Huang, J. Alchemical transformations and beyond: Recent advances and real-world applications of free energy calculations in drug discovery. *J. Chem. Inf. Model.* **2024**, *64*, 7214−7237.

(5) Shirts, M. R.; Mobley, D. L.; Brown, S. P. Free-energy calculations in structure-based drug design. *Drug Design* **2010**, *1*, 61−86.

(6) Cournia, Z.; Allen, B. K.; Beuming, T.; Pearlman, D. A.; Radak, B. K.; Sherman, W. Rigorous free energy simulations in virtual screening. *J. Chem. Inf. Model.* **2020**, *60*, 4153−4169.

(7) Rickman, J.; LeSar, R. Free-energy calculations in materials research. *Annu. Rev. Mater. Res.* **2002**, *32*, 195−217.

(8) Yang, L.; Sun, Y.; Ye, Z.; Zhang, F.; Mendelev, M.; Wang, C.; Ho, K. A self-contained algorithm for determination of solid-liquid equilibria in an alloy system. *Comput. Mater. Sci.* **2018**, *150*, 353−357.

(9) Cheng, B.; Ceriotti, M. Computing the absolute Gibbs free energy in atomistic simulations: Applications to defects in solids. *Phys. Rev. B* **2018**, *97*, 054102.

(10) Gambino, D.; Klarbring, J.; Alling, B. Phase stability of Fe from first principles: Atomistic spin dynamics coupled with ab initio molecular dynamics simulations and thermodynamic integration. *Phys. Rev. B* **2023**, *107*, 014102.

(11) Nam, J.; Peng, J.; Gómez-Bombarelli, R. Interpolation and differentiation of alchemical degrees of freedom in machine learning interatomic potentials. *Nat. Commun.* **2025**, *16*, 4350.

(12) Mey, A. S. J. S.; Allen, B. K.; Bruce Macdonald, H. E.; Chodera, J. D.; Hahn, D. F.; Kuhn, M.; Michel, J.; Mobley, D. L.; Naden, L. N.; Prasad, S.; et al. Best practices for alchemical free energy calculations [article v1. 0]. *Living journal of computational molecular science* **2020**, *2*, 18378.

(13) Klimovich, P. V.; Shirts, M. R.; Mobley, D. L. Guidelines for the analysis of free energy calculations. *J. Comput.-Aided Mol. Des.* **2015**, *29*, 397−411.

(14) Boulanger, E.; Huang, L.; Rupakheti, C.; MacKerell Jr, A. D.; Roux, B. Optimized Lennard-Jones parameters for druglike small molecules. *J. Chem. Theory Comput.* **2018**, *14*, 3121−3131.

(15) Jämbeck, J. P.; Mocci, F.; Lyubartsev, A. P.; Laaksonen, A. Partial atomic charges and their impact on the free energy of solvation. *J. Comput. Chem.* **2013**, *34*, 187−197.

(16) Mobley, D. L.; Dumont, E.; Chodera, J. D.; Dill, K. A. Comparison of charge models for fixed-charge force fields: small-molecule hydration free energies in explicit solvent. *J. Phys. Chem. B* **2007**, *111*, 2242−2254.

(17) Riquelme, M.; Lara, A.; Mobley, D. L.; Verstraelen, T.; Matamala, A. R.; Vohringer-Martinez, E. Hydration free energies in the FreeSolv database calculated with polarized iterative Hirshfeld charges. *J. Chem. Inf. Model.* **2018**, *58*, 1779−1797.

(18) Dodda, L. S.; Vilseck, J. Z.; Tirado-Rives, J.; Jorgensen, W. L. 1.14* CM1A-LBCC: localized bond-charge corrected CM1A charges for condensed-phase simulations. *J. Phys. Chem. B* **2017**, *121*, 3864−3870.
(19) Reynolds, C. A.; Essex, J. W.; Graham Richards, W. Errors in free-energy perturbation calculations due to neglecting the conformational variation of atomic charges. *Chem. Phys. Lett.* **1992**, *199*, 257−260.
(20) Osato, M.; Baumann, H. M.; Huang, J.; Alibay, I.; Mobley, D. L. Evaluating the Functional Importance of Conformer-Dependent Atomic Partial Charge Assignment. *J. Comput. Chem.* **2025**, *46*, No. e70112.
(21) Harry Moore, J.; Cole, D. J.; Csányi, G. Computing Solvation Free Energies of Small Molecules with Experimental Accuracy. *J. Am. Chem. Soc.* **2026**, *148*, 4928−4937.
(22) Batatia, I.; Csányi, G.; Kovacs, D. P.; Ortner, C.; Simm, G. MACE: Higher order equivariant message passing neural networks for fast and accurate force fields. *Advances in neural information processing systems* 2022, *35*, 11423−11436.
(23) Kovács, D. P.; Moore, J. H.; Browning, N. J.; Batatia, I.; Horton, J. T.; Pu, Y.; Kapil, V.; Witt, W. C.; Magdau, I.-B.; Cole, D. J.; et al. Mace-off: Short-range transferable machine learning force fields for organic molecules. *J. Am. Chem. Soc.* **2025**, *147*, 17598−17611.
(24) Mobley, D. L.; Guthrie, J. P. FreeSolv: a database of experimental and calculated hydration free energies, with input files. *J. Comput.-Aided Mol. Des.* **2014**, *28*, 711−720.
(25) Wu, Z.; Ramsundar, B.; Feinberg, E. N.; Gomes, J.; Geniesse, C.; Pappu, A. S.; Leswing, K.; Pande, V. MoleculeNet: a benchmark for molecular machine learning. *Chem. Sci.* **2018**, *9*, 513−530.
(26) Lim, H.; Jung, Y. MLSolvA: solvation free energy prediction from pairwise atomistic interactions by machine learning. *J. Cheminf.* **2021**, *13*, 56.
(27) Low, K.; Coote, M. L.; Izgorodina, E. I. Explainable solvation free energy prediction combining graph neural networks with chemical intuition. *J. Chem. Inf. Model.* **2022**, *62*, 5457−5470.
(28) Alibakhshi, A.; Hartke, B. Improved prediction of solvation free energies by machine-learning polarizable continuum solvation model. *Nat. Commun.* **2021**, *12*, 3584.
(29) Chung, Y.; Vermeire, F. H.; Wu, H.; Walker, P. J.; Abraham, M. H.; Green, W. H. Group contribution and machine learning approaches to predict Abraham solute parameters, solvation free energy, and solvation enthalpy. *J. Chem. Inf. Model.* **2022**, *62*, 433−446.
(30) Röcken, S.; Burnet, A. F.; Zavadlav, J. Predicting solvation free energies with an implicit solvent machine learning potential. *J. Chem. Phys.* **2024**, *161*, 234101.
(31) Wittmann, L.; Selzer, C. E.; Grimme, S. A diverse and chemically relevant solvation model benchmark set with flexible molecules and conformer ensembles. *Chem. Sci.* **2025**, *16*, 22976−22995.
(32) Bayly, C. I.; Cieplak, P.; Cornell, W.; Kollman, P. A. A well-behaved electrostatic potential based method using charge restraints for deriving atomic charges: the RESP model. *J. Phys. Chem.* **1993**, *97*, 10269−10280.
(33) Woods, R.; Chappelle, R. Restrained electrostatic potential atomic partial charges for condensed-phase simulations of carbohydrates. *J. Mol. Struct.:THEOCHEM* **2000**, *527*, 149−156.
(34) Jakalian, A.; Bush, B. L.; Jack, D. B.; Bayly, C. I. Fast, efficient generation of high-quality atomic charges. AM1-BCC model: I. Method. *J. Comput. Chem.* **2000**, *21*, 132−146.
(35) Jakalian, A.; Jack, D. B.; Bayly, C. I. Fast, efficient generation of high-quality atomic charges. AM1-BCC model: II. Parameterization and validation. *J. Comput. Chem.* **2002**, *23*, 1623−1641.
(36) Dewar, M. J.; Zoebisch, E. G.; Healy, E. F.; Stewart, J. J. Development and use of quantum mechanical molecular models. 76. AM1: a new general purpose quantum mechanical molecular model. *J. Am. Chem. Soc.* **1985**, *107*, 3902−3909.
(37) Su, Q.; Zhang, H.; Gou, Q.; Sun, H.; Fang, M.; Zhang, X.; Hu, R.; Kang, Y.; Hsieh, C.-Y.; Wang, J.; et al. others LumiCharge: Spherical Harmonic Convolutional Networks for Atomic Charge Prediction in Drug Discovery. *J. Phys. Chem. Lett.* **2025**, *16*, 6334−6344.
(38) Wang, J.; Cao, D.; Tang, C.; Xu, L.; He, Q.; Yang, B.; Chen, X.; Sun, H.; Hou, T. DeepAtomicCharge: a new graph convolutional network-based architecture for accurate prediction of atomic charges. *Briefings Bioinf.* **2021**, *22*, bbaa183.
(39) Wang, Y.; Pulido, I.; Takaba, K.; Kaminow, B.; Scheen, J.; Wang, L.; Chodera, J. D. EspalomaCharge: Machine learning-enabled ultrafast partial charge assignment. *J. Phys. Chem. A* **2024**, *128*, 4160−4167.
(40) Chen, T.; Guestrin, C. Xgboost: A scalable tree boosting system. In *Proceedings of the 22nd Acm Sigkdd International Conference on Knowledge Discovery and Data Mining*, 2016; pp 785−794.
(41) Wang, J.; Cao, D.; Tang, C.; Chen, X.; Sun, H.; Hou, T. Fast and accurate prediction of partial charges using Atom-Path-Descriptor-based machine learning. *Bioinformatics* **2020**, *36*, 4721−4728.
(42) Plé, T.; Lagardère, L.; Piquemal, J.-P. Force-field-enhanced neural network interactions: from local equivariant embedding to atom-in-molecule properties and long-range effects. *Chem. Sci.* **2023**, *14*, 12554−12569.
(43) Musaelian, A.; Batzner, S.; Johansson, A.; Sun, L.; Owen, C. J.; Kornbluth, M.; Kozinsky, B. Learning local equivariant representations for large-scale atomistic dynamics. *Nat. Commun.* **2023**, *14*, 579.
(44) Wang, J.; Wolf, R. M.; Caldwell, J. W.; Kollman, P. A.; Case, D. A. Development and testing of a general amber force field. *J. Comput. Chem.* **2004**, *25*, 1157−1174.
(45) Basma, M.; Sundara, S.; Çalgan, D.; Vernali, T.; Woods, R. J. Solvated ensemble averaging in the calculation of partial atomic charges. *J. Comput. Chem.* **2001**, *22*, 1125−1137.
(46) Reynolds, C. A.; Essex, J. W.; Richards, W. G. Atomic charges for variable molecular conformations. *J. Am. Chem. Soc.* **1992**, *114*, 9075−9079.
(47) Singh, U. C.; Kollman, P. A. An approach to computing electrostatic charges for molecules. *J. Comput. Chem.* **1984**, *5*, 129−145.
(48) Besler, B. H.; Merz Jr, K. M.; Kollman, P. A. Atomic charges derived from semiempirical methods. *J. Comput. Chem.* **1990**, *11*, 431−439.
(49) Frisch, M. J.; et al. *Gaussian 16*; Revision C.01; Gaussian Inc.: Wallingford CT, 2016.
(50) Adamo, C.; Barone, V. Toward reliable density functional methods without adjustable parameters: The PBE0 model. *J. Chem. Phys.* **1999**, *110*, 6158−6170.
(51) Ernzerhof, M.; Scuseria, G. E. Assessment of the Perdew−Burke−Ernzerhof exchange-correlation functional. *J. Chem. Phys.* **1999**, *110*, 5029−5036.
(52) Weigend, F.; Ahlrichs, R. Balanced basis sets of split valence, triple zeta valence and quadruple zeta valence quality for H to Rn: Design and assessment of accuracy. *Phys. Chem. Chem. Phys.* **2005**, *7*, 3297−3305.
(53) Weigend, F. Accurate Coulomb-fitting basis sets for H to Rn. *Phys. Chem. Chem. Phys.* **2006**, *8*, 1057−1065.
(54) Grimme, S.; Ehrlich, S.; Goerigk, L. Effect of the damping function in dispersion corrected density functional theory. *J. Comput. Chem.* **2011**, *32*, 1456−1465.
(55) Petersson, a.; Bennett, A.; Tensfeldt, T. G.; Al-Laham, M. A.; Shirley, W. A.; Mantzaris, J. A complete basis set model chemistry. I. The total energies of closed-shell atoms and hydrides of the first-row elements. *J. Chem. Phys.* **1988**, *89*, 2193−2218.
(56) Petersson, G.; Al-Laham, M. A. A complete basis set model chemistry. II. Open-shell systems and the total energies of the first-row atoms. *J. Chem. Phys.* **1991**, *94*, 6081−6090.
(57) Case, D. A.; Aktulga, H. M.; Belfon, K.; Cerutti, D. S.; Cisneros, G. A.; Cruzeiro, V. W. D.; Forouzesh, N.; Giese, T. J.; G"otz, A. W.; Gohlke, H.; et al. AmberTools. *J. Chem. Inf. Model.* **2023**, *63*, 6183−6191.
(58) Mobley, D. L.; Bannan, C. C.; Rizzi, A.; Bayly, C. I.; Chodera, J. D.; Lim, V. T.; Lim, N. M.; Beauchamp, K. A.; Slochower, D. R.; Shirts, M. R.; et al. Escaping atom types in force fields using direct chemical perception. *J. Chem. Theory Comput.* **2018**, *14*, 6076−6092.
(59) Wagner, J. et al. *openforcefield/openff-toolkit: 0.16.4 minor feature and bugfix release*; Version 0.16.4; Zenodo 2024.

https://doi.org/10.1021/acs.jctc.5c02086
J. Chem. Theory Comput. 2026, 22, 4481−4492

(60) Medrano Sandonas, L.; Van Rompaey, D.; Fallani, A.; Hilfiker, M.; Hahn, D.; Perez-Benito, L.; Verhoeven, J.; Tresadern, G.; Kurt Wegner, J.; Ceulemans, H.; et al. Dataset for quantum-mechanical exploration of conformers and solvent effects in large drug-like molecules. *Sci. Data* **2024**, *11*, 742.
(61) Hjorth Larsen, A.; et al. The atomic simulation environment-a Python library for working with atoms. *J. Phys.: Condens. Matter* **2017**, *29*, 273002.
(62) Akiba, T.; Sano, S.; Yanase, T.; Ohta, T.; Koyama, M. O. A Next-Generation Hyperparameter Optimization Framework. In *The 25th ACM SIGKDD International Conference on Knowledge Discovery & Data Mining*, 2019; pp 2623−2631.
(63) Eastman, P.; Galvelis, R.; Peláez, R. P.; Abreu, C. R.; Farr, S. E.; Gallicchio, E.; Gorenko, A.; Henry, M. M.; Hu, F.; Huang, J.; et al. OpenMM 8: molecular dynamics simulation with machine learning potentials. *J. Phys. Chem. B* **2023**, *128*, 109−116.
(64) Landrum, G. et al. *rdkit/rdkit: 2023_03_3 (Q1 2023) Release*; Zenodo 2023.
(65) Rappe, A. K.; Casewit, C. J.; Colwell, K. S.; Goddard, W. A.; Skiff, W. M. UFF, a full periodic table force field for molecular mechanics and molecular dynamics simulations. *J. Am. Chem. Soc.* **1992**, *114*, 10024−10035.
(66) Gowers, R. J.; Alibay, I.; Swenson, D. W.; Henry, M. M.; Ries, B.; Baumann, H. M.; Eastwood, J. R. B.; Mitchell, J. A.; Dotson, D.; Horton, J. T.; Thompson, M. *The Open Free Energy library*; Zenodo. 2024.
(67) Jorgensen, W. L.; Chandrasekhar, J.; Madura, J. D.; Impey, R. W.; Klein, M. L. Comparison of simple potential functions for simulating liquid water. *J. Chem. Phys.* **1983**, *79*, 926−935.
(68) Darden, T.; York, D.; Pedersen, L. others Particle mesh Ewald: An N log (N) method for Ewald sums in large systems. *J. Chem. Phys.* **1993**, *98*, 10089.
(69) Shirts, M. R.; Chodera, J. D. Statistically optimal analysis of samples from multiple equilibrium states. *J. Chem. Phys.* **2008**, *129*, 124105.
(70) Pedregosa, F.; Varoquaux, G.; Gramfort, A.; Michel, V.; Thirion, B.; Grisel, O.; Blondel, M.; Prettenhofer, P.; Weiss, R.; Dubourg, V.; et al. Scikit-learn: Machine learning in Python. *J. Mach. Learn. Res.* **2011**, *12*, 2825−2830.
(71) O'Boyle, N. M.; Banck, M.; James, C. A.; Morley, C.; Vandermeersch, T.; Hutchison, G. R. Open Babel: An open chemical toolbox. *J. Cheminf.* **2011**, *3*, 33.
(72) Rocklin, G. J.; Mobley, D. L.; Dill, K. A.; Hünenberger, P. H. Calculating the binding free energies of charged species based on explicit-solvent simulations employing lattice-sum methods: An accurate correction scheme for electrostatic finite-size effects. *J. Chem. Phys.* **2013**, *139*, 184103.
(73) Mahalanobis, P. C. On the generalized distance in statistics. *Sankhyā: The Indian Journal of Statistics, Series A* **2008**, *80*, S1−S7.
(74) Huang, L.; Roux, B. Automated force field parameterization for nonpolarizable and polarizable atomic models based on ab initio target data. *J. Chem. Theory Comput.* **2013**, *9*, 3543−3556.
(75) Mobley, D. L.; Bayly, C. I.; Cooper, M. D.; Dill, K. A. Predictions of hydration free energies from all-atom molecular dynamics simulations. *J. Phys. Chem. B* **2009**, *113*, 4533−4537.
(76) Muddana, H. S.; Sapra, N. V.; Fenley, A. T.; Gilson, M. K. The SAMPL4 hydration challenge: evaluation of partial charge sets with explicit-water molecular dynamics simulations. *J. Comput.-Aided Mol. Des.* **2014**, *28*, 277−287.

https://doi.org/10.1021/acs.jctc.5c02086
J. Chem. Theory Comput. 2026, 22, 4481−4492